

Multi-spectrum to RGB with Direct Structure-tensor Reconstruction

Takashi Shibata^{1,2}, Masayuki Tanaka¹, Masatoshi Okutomi¹;

¹ Tokyo Institute of Technology; Tokyo, Japan

² NEC corporation; Kanagawa, Japan

Abstract

This paper proposes a novel multi-spectrum to RGB method with direct structure-tensor reconstruction. The goal of the proposed method is to generate a fused color image which preserves structure-tensor of the original multispectral image while keeping naturalistic color of a reference RGB image. Existing multi-spectrum to RGB methods generate the fused image by sequential pipeline that consists of fused-gradient estimation and reintegration. The existing sequential pipeline tends to generate the fused image whose structure-tensor is deviated from the structure-tensor of the original multispectral image. Contrary to the existing sequential pipeline, the proposed method generates the fused image directly with the structure-tensor of the original multispectral image by minimizing an energy which consists of the structure-tensor term and the reference color constraint term. The proposed direct structure-tensor reconstruction enables us to preserve the structure-tensor of the multispectral image while keeping the naturalistic color of the reference RGB image. The experimental results on multispectral images including visible and NIR images show that the proposed method outperforms the existing methods in terms of not only image quality but also quantitative evaluations.

Introduction

Multispectral imaging has various applications including remote sensing and biometrics [6, 23]. Recent advances in computational photography techniques (e.g. designing color filter array [30, 18, 24, 25] or beam-splitter [47]) have provided an easy way to acquire a multispectral image. To analyze the multispectral image by human using a standard display, a multi-spectrum to RGB technique which converts the multispectral image to a single image is required. This technique is called image fusion, the goal of which is to generate an image that contains an important feature of the multispectral image while keeping naturalistic color of the multispectral image.

Traditional image fusion methods for generating a gray-scale image are based on pyramidal decompositions such as the wavelet-transform [21], the Gaussian and the Laplacian pyramid [44, 27] as shown in Table. 1. The existing methods, however, cannot preserve the feature of the multispectral image sufficiently because a single-band is selected from the multispectral image pixel-by-pixel in the decomposed domain, i.e. the feature of the other bands is discarded. Dimensionality reduction techniques such as PCA [45, 31], ISOMAP [9] are also applied to generate a fused-image to preserve the feature of the multispectral image. Although these methods are effective to contain the feature of the multispectral image, the fused image with gray-scale

or false-color is generated.

Variation-based methods are also proposed to preserve the feature of the multispectral image using differential-geometry [38, 28]. Socolinsky first presented the variation-based method for generating a gray-scale image using the structure-tensor which represents geometric structure of the multispectral image [38].

Motivated by the existing variation-based methods [38, 28], Connah et al. recently proposed “Spectral Edge Image Fusion” [8] to generate a naturalistic color image from the multispectral image. The pipeline of Connah’s method consists of fused-gradient estimation and reintegration as shown in Fig. 1 (a). In the fused-gradient estimation, Connah’s method can generate the gradient which not only preserves the structure-tensor of the multispectral image but also keeps the naturalistic color of the reference RGB image. However, after reintegration, the structure-tensor of the fused image tends to deviate from the structure-tensor of the multispectral image because there is no constraint to preserve the structure-tensor of the multispectral image at the reintegration.

The goal of the proposed method is to generate the fused RGB image which preserves the structure-tensor of the multispectral image while keeping the natural color of the reference RGB image. The proposed method generates the fused RGB image by direct reconstruction from the structure-tensor of the multispectral image and the reference RGB image. The pipeline of the proposed method is shown in Fig. 1 (b). Our method directly reconstructs the fused image with the structure-tensor of the multispectral image by minimizing the energy which consists of the structure-tensor term and the reference color constraints.

Novelties of this paper include: 1) We propose the novel method of converting multi-spectrum to RGB with direct structure-tensor reconstruction, while the existing method is sequential. 2) To accomplish this converting, the novel energy composed of the structure-tensor term and the reference color constraints is presented, while the existing method cannot reflect natural color of the reference RGB image.

Related works

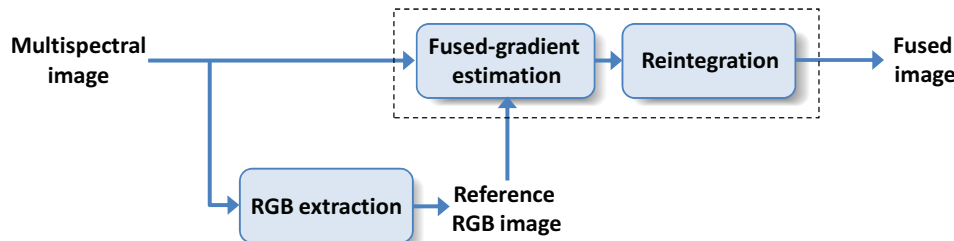
Image fusion

Image fusion is a technique for generating an informative single image by combining multiple input images. This technique is used in various applications such as image analysis and machine recognition.

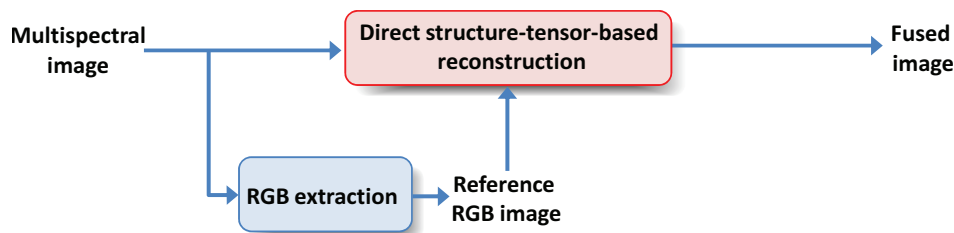
Traditional image fusion methods for generating a gray-scale image are based on pyramidal decompositions such as the wavelet-transform [21], the Gaussian and the Laplacian pyra-

Table 1. Comparison of existing methods and proposed method

Method	Feature of multispectral image	Color of fused result
Pyramidal decomposition approach [44, 27, 45, 31, 46]	Transformed domain	- (gray-scale)
Dimensionality reduction approach [45, 31, 9]	Sub-space (e.g. PCA, ISOMAP)	False color
Variation-based for generating gray-scale image [38, 28]	Structure-tensor (sequential)	- (gray-scale)
Spectral Edge Image Fusion [8]	Structure-tensor (sequential)	Natural color
Proposed method	Structure-tensor (directed)	Natural color



(a) Pipeline of existing method "Spectral Edge Image Fusion [8]": Sequential approach



(b) Pipeline of proposed method method: Direct approach

Figure 1. Pipeline of existing method and proposed method. The pipeline of the existing method [8]) consists of the two steps: 1) fused-gradient estimation, and 2) reintegration. In the existing method, the fused-gradient estimation and the reintegration are sequentially processed as shown in the dotted box. The problem is that the structure-tensor of the fused image tends to deviate from the structure-tensor of the multispectral image after the reintegration. Contrary to the existing sequential pipeline, the proposed method generates the fused image by the direct structure-tensor construction. The direct approach enables us to preserve the structure-tensor of the multispectral image while keeping natural color using the reference RGB image.

mid [44, 27], and the contourlet transform [46]. In the pyramidal decomposition methods, the fused image is generated by combining pixel-by-pixel in the transformed domains. Although the pyramidal decomposition methods are computationally effective, the methods tends to generate artifacts in a smooth region. To restrain the artifacts, the sophisticated image fusion methods introduces the smoothness constraints based on the generalized random walks [33], the Markov Random Filed [42, 37, 36] and the guided filter [22]. Another issue on the existing pyramidal decomposition methods [21, 44, 27, 46] is that the methods cannot preserve the feature of the multispectral image sufficiently.

Dimensionality reduction techniques such as PCA [45, 31], ISOMAP [9] are also applied to generate the fused-image to preserve the feature of the multispectral image. Although these methods are effective to contain the feature of the multispectral image, the fused image with gray-scale or false-color is generated.

Another approach of image fusion method is Variation-based methods [8, 12, 15, 38, 28]. Variation-based methods can preserve the feature of the multispectral image using differential-geometry [38, 28]. Socolinsky first presented the variation-based method for generating a gray-scale image using the structure-

tensor which represents geometric structure of the multispectral image [38]. Motivated by the existing variation-based methods [38, 28], "Spectral Edge Image Fusion" [8] and its improved version [12] is proposed to generate a naturalistic color image from the multispectral image.

Gradient-domain image reconstruction

The gradient-domain image reconstruction is effective for various applications in computer graphics and image processing field. For example, image editing framework called "Poisson image editing" was also presented by Perez [26]. Image fusion algorithms in the gradient-domain were proposed [1, 8, 29, 42, 37, 36]. Sun. et al. also proposed the image matting algorithm based on Poisson equation [40]. Image inpainting method based on the gradient-domain were also presented to reconstruct the structure and the texture [32, 34, 35, 41]. Other applications in gradient-domain include seamless image stitching [48, 16, 20], HDR tone mapping [10, 4], surface reconstruction [3, 17, 2, 13], color interpolation [19, 4], and color-to-gray mapping [11, 14].

As described later, the proposed method reconstructs the fused RGB image using the fast Poisson reconstruction [43]

which is the same manner of the Frankot's approach [3, 13]. In that sense, the proposed method is the extended version of gradient-domain image reconstruction framework to preserve the structure-tensor of the input image.

Proposed method

Our method directly reconstructs the fused image with the structure-tensor of the multispectral image by minimizing the energy which consists of the structure-tensor term and the reference color constraints. Here, the reference RGB image is obtained by selecting the corresponding band of each channel from the multispectral image. The structure-tensor of the multispectral image which represents the geometric structure of the multispectral image is defined as

$$G_i := (\nabla H_i)^T (\nabla H_i), \quad (1)$$

where G_i and ∂H_i are the structure-tensor of the multispectral image and the gradient of the multispectral image at i -th pixel. Here, the multispectral image consists of M band, and the gradient ∂H_i is defined as

$$\nabla \mathbf{H}_i = \begin{pmatrix} \partial_x H_i^1 & \partial_y H_i^1 \\ \vdots & \vdots \\ \partial_x H_i^M & \partial_y H_i^M \end{pmatrix}. \quad (2)$$

The direct structure-tensor-based reconstruction generates the fused image from the structure-tensor of the multispectral image G_i and the reference RGB image so that the structure-tensor of the multispectral image G_i is preserved while the color of the fused image is similar to that of the reference RGB image. Contrary to the existing sequential pipeline, the proposed method directly generates the fused image by minimizing the energy. In the proposed method, to preserve the the structure-tensor of the multispectral image G_i , we introduce a structure-tensor fidelity term which penalizes the structure-tensor differences between the fused image and the multispectral image. On the other hand, the reference color constraint is introduced, so that the color of the fused image is similar to that of the reference RGB image. Specifically, the energy to reconstruct the fused image is given by

$$E(\{\mathbf{R}_i\}) = \sum_i \|(\nabla \mathbf{R}_i)^T (\nabla \mathbf{R}_i) - \mathbf{G}_i\|_F^2 + \alpha \sum_i \|\nabla \mathbf{R}_i - \nabla \tilde{\mathbf{R}}_i\|_F^2 + \varepsilon \sum_i \|\mathbf{R}_i - \tilde{\mathbf{R}}_i\|_2^2, \quad (3)$$

where \mathbf{R}_i is the set of the RGB intensity of the fused image, $\tilde{\mathbf{R}}_i$ is the RGB intensity of the reference RGB image at i -th pixel, α and ε are the parameter to balance each term. In Eq. (3), the first term is the structure-tensor fidelity term. The second and third term represent the reference color constraint that penalize the residual between the color intensities of the fused image and the reference RGB image in the gradient and the color intensity domains.

The proposed energy can be effectively optimized using the quadratic relaxation [7, 39]. To optimize the energy in Eq. (3) by the quadratic relaxation, we rewrite the energy function by intro-

Algorithm 1 Minimize $\tilde{E}(\{\mathbf{R}_i\})$ in Eq. (3)

given α , β and ε
 $\mathbf{G}_i = (\nabla H_i)^T (\nabla H_i)$ using Eq. (1) and Eq. (2)
initialize $\{\mathbf{R}_i\} = \{\tilde{\mathbf{R}}_i\}$ and $\{\hat{\mathbf{R}}_i\} = \mathbf{R}_i$,
for $k = 0$ to K **do**
 $\{\hat{\mathbf{v}}_i\} = \arg \min_{\{\mathbf{v}_i\}} \tilde{E}_v(\{\mathbf{v}_i\} | \{\nabla \hat{\mathbf{R}}_i\})$ in Eq. (5)
 $\{\hat{\mathbf{R}}_i\} = \arg \min_{\{\mathbf{R}_i\}} \tilde{E}_R(\{\mathbf{R}_i\} | \{\hat{\mathbf{v}}_i\})$ in Eq. (6)
 $\beta \leftarrow \beta \times 2$
end for
return $\{\mathbf{R}_i\}$

ducing the slack variable \mathbf{v}_i as

$$\begin{aligned} \tilde{E}(\{\mathbf{R}_i\}, \mathbf{v}_i) &= \sum_i \|\mathbf{v}_i^T \mathbf{v}_i - \mathbf{G}_i\|_F^2 + \\ &\alpha \sum_i \|\nabla \tilde{\mathbf{R}}_i - \mathbf{v}_i\|_F^2 + \beta \sum_i \|\nabla \mathbf{R}_i - \mathbf{v}_i\|_F^2 + \varepsilon \sum_i \|\mathbf{R}_i - \tilde{\mathbf{R}}_i\|_2^2, \end{aligned} \quad (4)$$

where β is a parameter to control the relative strength of the third term. In the proposed method, β is incremented for each iteration. To minimize the energy $\tilde{E}(\{\mathbf{R}_i\}, \mathbf{v}_i)$ in Eq. (4), we update alternatively \mathbf{R}_i and \mathbf{v}_i . In the manner of the quadratic relaxation, \mathbf{R}_i is updated during fixing \mathbf{v}_i as $\hat{\mathbf{R}}_i$. On the other hand \mathbf{v}_i is updated during fixing \mathbf{R}_i as $\hat{\mathbf{v}}_i$. The energies for updating \mathbf{R}_i and \mathbf{v}_i are given by

$$\begin{aligned} \tilde{E}_v(\{\mathbf{v}_i\} | \{\nabla \hat{\mathbf{R}}_i\}) &= \sum_i \|\mathbf{v}_i^T \mathbf{v}_i - \mathbf{G}_i\|_F^2 \\ &+ \alpha \sum_i \|\nabla \tilde{\mathbf{R}}_i - \mathbf{v}_i\|_F^2 + \beta \sum_i \|\nabla \hat{\mathbf{R}}_i - \mathbf{v}_i\|_F^2, \end{aligned} \quad (5)$$

$$\tilde{E}_R(\{\mathbf{R}_i\} | \{\hat{\mathbf{v}}_i\}) = \beta \sum_i \|\nabla \mathbf{R}_i - \hat{\mathbf{v}}_i\|_F^2 + \varepsilon \sum_i \|\mathbf{R}_i - \tilde{\mathbf{R}}_i\|_2^2. \quad (6)$$

It is worthy noting that the combination of \mathbf{v}_i can be updated pixel-by-pixel independently by $\tilde{E}_v(\{\mathbf{v}_i\} | \{\nabla \hat{\mathbf{R}}_i\})$ while \mathbf{R}_i can be updated effectively by the fast Poisson reconstruction which is explained in Appendix. The pseudo code for minimizing $\tilde{E}(\{\mathbf{R}_i\})$ in Eq. (3) is shown in Algorithm 1.

Experiments

We conducted experiments¹ with the multispectral images including the visible and the NIR images[5] and satellite images². We implemented the existing methods [8] for comparison because the source code is not available.

Fig. 2 and Fig. 3 shows that the result on the multispectral image composed of the visible and the NIR. Again, Fig. 3 (b) shows that the PCA-based method [45] generates the false color. As shown in Fig. 4(c) and (d), although ‘‘Spectral Image Edge Fusion’’ [8] slightly improves the visibility at the haze region, the proposed method can generate the fused image with the high-visibility view by fusing the NIR. We evaluate the root-mean-square error (RMSE) between the structure-tensor of the results and that of the multispectral image \mathbf{G}_i . The RMSE of the re-

¹The additional results and information will be available at <http://www.ok.ctrl.titech.ac.jp/res/CID>

²NASA: Landsat imagery, <http://glof.umd.edu/data/gls/>

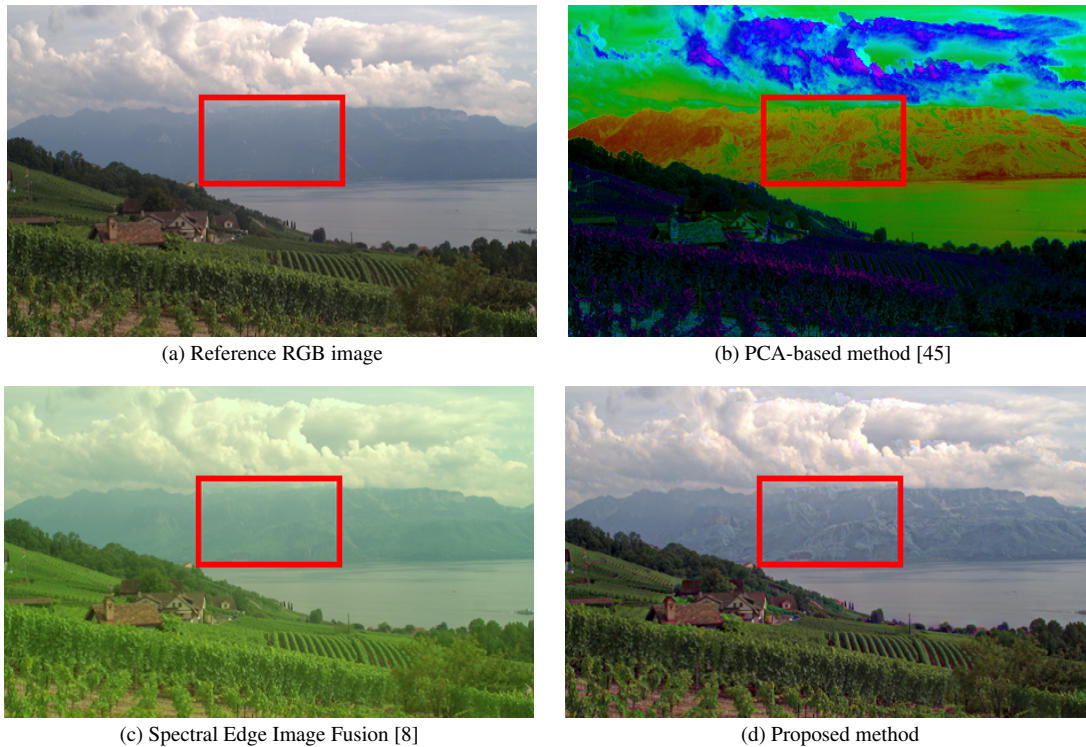


Figure 2. Result on multispectral image (visible and NIR image pair).

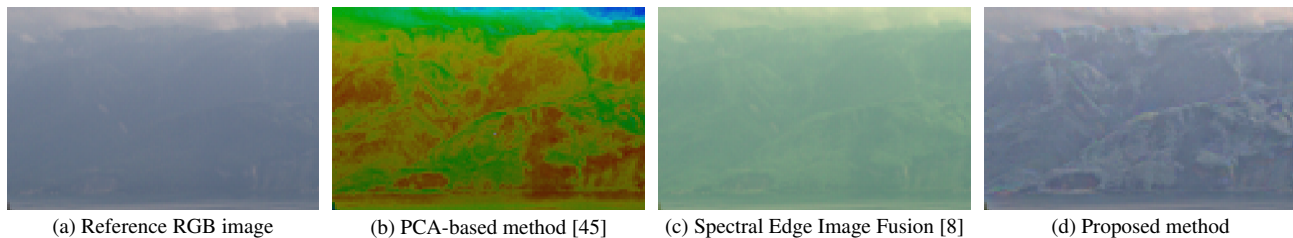


Figure 3. Result on multispectral image (close-ups).

sults by proposed method and “Spectral Image Edge Fusion” [8] are 0.00123 and 0.00659, respectively. This result shows that the proposed method can preserve the structure-tensor of the multispectral image than the existing method quantitatively.

Finally, we show the results on satellite images composed of seven-band. As shown in Fig. 4 and Fig. 5, the proposed method can improve the visibility by preserving the structure-tensor of the multispectral image while keeping the natural color of the reference RGB image.

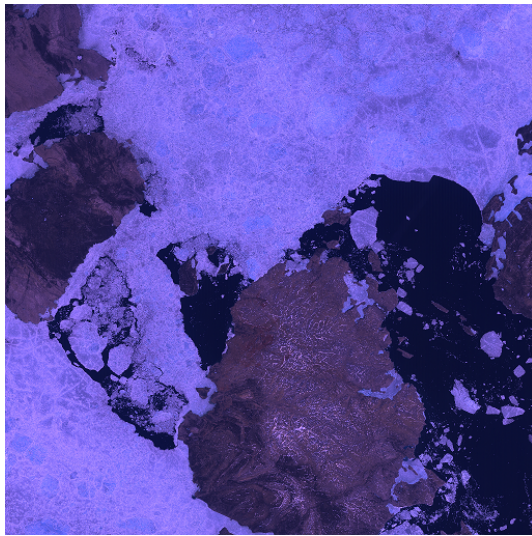
Conclusion

The novel multi-spectrum to RGB method with direct structure-tensor reconstruction has been proposed. The proposed method generates the fused image directly with the structure-tensor of the original multispectral image by minimizing an energy which consists of the structure-tensor term and the reference color constraint term. The proposed direct structure-tensor reconstruction enables us to preserve the structure-tensor of the multispectral image while keeping the naturalistic color of the reference RGB image. The experimental results on multispectral im-

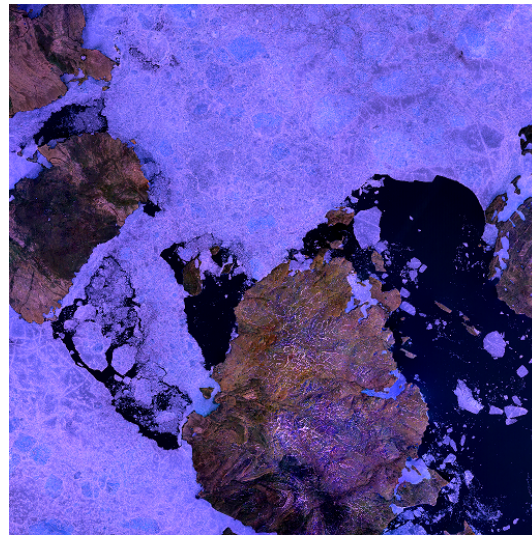
ages including visible and NIR images showed that the proposed method outperforms the existing methods in terms of not only image quality but also quantitative evaluations.

References

- [1] A. Agarwala, M. Dontcheva, M. Agrawala, S. Drucker, A. Colburn, B. Curless, D. Salesin, and M. Cohen. Interactive digital photomontage. *ACM Trans. on Graphics (TOG)*, 23(3):294–302, 2004.
- [2] A. Agrawal, R. Chellappa, and R. Raskar. An algebraic approach to surface reconstruction from gradient fields. *Proc. of IEEE Int. Conf. on Computer Vision (ICCV)*, 1:174–181, 2005.
- [3] A. Agrawal, R. Raskar, and R. Chellappa. What is the range of surface reconstructions from a gradient field? *Proc. of European Conf. on Computer Vision (ECCV)*, pages 578–591, 2006.
- [4] P. Bhat, C. L. Zitnick, M. Cohen, and B. Curless. Gradientshop: A gradient-domain optimization framework for image and video filtering. *ACM Trans. on Graphics (TOG)*, 29(2):10, 2010.
- [5] M. Brown and S. Süsstrunk. Multi-spectral sift for scene category recognition. pages 177–184, 2011.
- [6] J. B. Campbell. Introduction to remote sensing. pages 177–184,



(a) Reference RGB image



(b) Proposed method

Figure 4. Result on satellite multispectral image (Landsat, seven-band).



(a) Reference RGB image



(b) Proposed method

Figure 5. Result on satellite multispectral image (Landsat, seven-band).

- 2002.
- [7] A. Chambolle. An algorithm for total variation minimization and applications. *Journal of Mathematical imaging and vision*, 20(1-2):89–97, 2004.
 - [8] D. Connah, M. S. Drew, and G. D. Finlayson. Spectral edge image fusion: Theory and applications. *Proc. of European Conf. on Computer Vision (ECCV)*, pages 65–80, 2014.
 - [9] M. Cui, J. Hu, A. Razdan, and P. Wonka. Color-to-gray conversion using isomap. *The Visual Computer*, 26(11):1349–1360, 2010.
 - [10] R. Fattal, D. Lischinski, and M. Werman. Gradient domain high dynamic range compression. *ACM Trans. on Graphics (TOG)*, 21(3):249–256, 2002.
 - [11] G. D. Finlayson, D. Connah, and M. S. Drew. Lookup-table-based gradient field reconstruction. *IEEE Trans. on Image Processing*, 20(10):2827–2836, 2011.
 - [12] G. D. Finlayson and A. E. Hayes. Iterative spectral edge image fusion. *Proc. of Color and Imaging Conference (CIC)*, 2015(1):41–45, 2015.
 - [13] R. T. Frankot and R. Chellappa. A method for enforcing integrability in shape from shading algorithms. *IEEE Trans. on Pattern Analysis and Machine Intelligence*, 10(4):439–451, 1988.
 - [14] A. A. Gooch, S. C. Olsen, J. Tumblin, and B. Gooch. Color2gray: salience-preserving color removal. *ACM Trans. on Graphics (TOG)*, 24(3):634–639, 2005.
 - [15] A. E. Hayes, G. D. Finlayson, and R. Montagna. Rgb-nir color image fusion: metric and psychophysical experiments. *IS&T/SPIE Electronic Imaging*, pages 93960U–93960U, 2015.
 - [16] J. Jia, J. Sun, C.-K. Tang, and H.-Y. Shum. Drag-and-drop pasting. *ACM Transactions on Graphics (TOG)*, 25(3):631–637, 2006.
 - [17] M. Kazhdan, M. Bolitho, and H. Hoppe. Poisson surface reconstruction. *Proc. of the fourth Eurographics symposium on Geometry processing*, 7, 2006.
 - [18] D. Kiku, Y. Monno, M. Tanaka, and M. Okutomi. Simultaneous capturing of RGB and additional band images using hybrid color filter array. *Proc. of SPIE*, pages 90230V–1–9, 2014.
 - [19] A. Levin, D. Lischinski, and Y. Weiss. Colorization using optimiza-

- tion. *ACM Trans. on Graphics (TOG)*, 23(3):689–694, 2004.
- [20] A. Levin, A. Zomet, S. Peleg, and Y. Weiss. Seamless image stitching in the gradient domain. *Proc. of European Conf. on Computer Vision (ECCV)*, pages 377–389, 2004.
- [21] H. Li, B. S. Manjunath, and S. K. Mitra. Multisensor image fusion using the wavelet transform. *Proc. of IEEE Int. Conf. on Graphical models and image processing*, 57(3):235–245, 1995.
- [22] S. Li, X. Kang, and J. Hu. Image fusion with guided filtering. *IEEE Trans. on Image Processing*, 22(7):2864–2875, 2013.
- [23] S. Z. Li, R. F. Chu, S. C. Liao, and L. Zhang. Illumination invariant face recognition using near-infrared images. *IEEE Trans. on Pattern Analysis and Machine Intelligence*, 29(4):627–639, 2007.
- [24] Y. M. Lu, C. Fredembach, M. Vetterli, and S. Süsstrunk. Designing color filter arrays for the joint capture of visible and near-infrared images. *Proc. of IEEE Int. Conf. on Image Processing (ICIP)*, pages 3797–3800, 2009.
- [25] Y. Monno, S. Kikuchi, M. Tanaka, and M. Okutomi. A practical one-shot multispectral imaging system using a single image sensor. *IEEE Trans. on Image Processing*, 24(10):3048–3059, 2015.
- [26] P. Pérez, M. Gangnet, and A. Blake. Poisson image editing. *ACM Trans. on Graphics (TOG)*, 22(3):313–318, 2003.
- [27] V. S. Petrovic and C. S. Xydeas. Gradient-based multiresolution image fusion. *IEEE Trans. on Image Processing*, 13(2):228–237, 2004.
- [28] G. Piella. Image fusion for enhanced visualization: A variational approach. *International Journal of Computer Vision*, 83(1):1–11, 2009.
- [29] R. Raskar, A. Ilie, and J. Yu. Image fusion for context enhancement and video surrealism. *Proc. of Int. Symp. on Non-Photorealistic Animation and Rendering (NPAR)*, (7):85 – 152, 2004.
- [30] Z. Sadeghipoor, Y. M. Lu, and S. Süsstrunk. Correlation-based joint acquisition and demosaicing of visible and near-infrared images. *Proc. of IEEE Int. Conf. on Image Processing (ICIP)*, pages 3226–3229, 2011.
- [31] J.-W. Seo and S. D. Kim. Novel pca-based color-to-gray image conversion. pages 2279–2283, 2013.
- [32] J. Shen, X. Jin, C. Zhou, and C. C. Wang. Gradient based image completion by solving the poisson equation. *Computers & Graphics*, 31(1):119–126, 2007.
- [33] R. Shen, I. Cheng, J. Shi, and A. Basu. Generalized random walks for fusion of multi-exposure images. *IEEE Trans. on Image Processing*, 20(12):3634–3646, 2011.
- [34] T. Shibata, A. Iketani, and S. Senda. Fast and structure-preserving inpainting based on probabilistic structure estimation. *Proc. of Machine Vision Applications (MVA)*, pages 22–25, 2011.
- [35] T. Shibata, A. Iketani, and S. Senda. Image inpainting based on probabilistic structure estimation. *Proc. of Asian Conf. on Computer Vision (ACCV)*, pages 109–120, 2011.
- [36] T. Shibata, M. Tanaka, and M. Okutomi. Unified image fusion based on application-adaptive importance measure. *Proc. of IEEE Int. Conf. on Image Processing (ICIP)*, 2015.
- [37] T. Shibata, M. Tanaka, and M. Okutomi. Visible and near-infrared image fusion based on visually salient area selection. *Proc. of SPIE Electrical Imaging*, pages 90230V–1–9, 2015.
- [38] D. Socolinsky, L. B. Wolff, et al. Multispectral image visualization through first-order fusion. *Image Processing, IEEE Transactions on*, 11(8):923–931, 2002.
- [39] F. Steinbrücker, T. Pock, and D. Cremers. Large displacement optical flow computation without warping. *Proc. of IEEE Int. Conf. on Computer Vision (ICCV)*, pages 1609–1614, 2009.
- [40] J. Sun, J. Jia, C.-K. Tang, and H.-Y. Shum. Poisson matting. *ACM Trans. on Graphics (ToG)*, 23(3):315–321, 2004.
- [41] J. Sun, L. Yuan, J. Jia, and H.-Y. Shum. Image completion with structure propagation. *ACM Trans. on Graphics (ToG)*, 24(3):861–868, 2005.
- [42] J. Sun, H. Zhu, Z. Xu, and C. Han. Poisson image fusion based on markov random field fusion model. *Information Fusion*, 14(3):241–254, 2013.
- [43] M. Tanaka, R. Kamiya, and M. Okutomi. Seamless image cloning by a closed form solution of a modified poisson problem. *Proc. of 5th ACM SIGGRAPH Conf. and Exhibit. on Computer Graphics and Interactive Techniques in Asia (SIGGRAPH Asia 2012)*, pages p.c08–0164–1–1, 2012.
- [44] A. Toet. Hierarchical image fusion. *Machine Vision and Applications*, 3(1):1–11, 1990.
- [45] J. S. Tyo, A. Konsolakis, D. Diersen, R. C. Olsen, et al. Principal-components-based display strategy for spectral imagery. *Geoscience and Remote Sensing, IEEE Transactions on*, 41(3):708–718, 2003.
- [46] B. Yang, S. Li, and F. Sun. Image fusion using nonsubsampling contourlet transform. *Proc. of IEEE Int. Conf. on Image and Graphics*, pages 719–724, 2007.
- [47] X. Zhang, T. Sim, and X. Miao. Enhancing photographs with near infra-red images. *Proc. of the Conf. on Computer Vision and Pattern Recognition (CVPR)*, pages 1–8, 2008.
- [48] A. Zomet, A. Levin, S. Peleg, and Y. Weiss. Seamless image stitching by minimizing false edges. *IEEE Trans. on Image Processing*, 15(4):969–977, 2006.

Appendix: Fast Poisson reconstruction

In this appendix, we present the detailed description of the computational effective gradient-domain image reconstruction algorithm which is the same manner of the Frankot’s approach [13, 3]³. In general, the optimization problem for the Poisson problem [26] is described as

$$\min_r \int_{\Omega} |\nabla r - \mathbf{v}|^2 d\Omega \quad \text{with} \quad r|_{\partial\Omega} = r^*|_{\partial\Omega}, \quad (7)$$

where r is the reconstructed image intensity, \mathbf{v} is the guidance gradient field, Ω is the target region (hole region), and $\partial\Omega$ is the boundary region between the target region and the source region. The solution of the optimization problem is obtained by solving the Poisson equation with the Dirichlet boundary condition:

$$\Delta r = \text{div} \mathbf{v} \quad \text{over} \quad \Omega \quad \text{with} \quad r|_{\partial\Omega} = r^*|_{\partial\Omega}, \quad (8)$$

where Δ is the Laplacian operator. In the Poisson image editing [26], the Poisson equation is solved by Gauss-Seidel method. Although the Poisson image editing is very effective for various applications, the Gauss-Seidel method requires large computational cost because the Gauss-Seidel method is an iterative technique. Further more, the Poisson image editing approach has a limitation which the color of the target region will be totally adapted to the source region.

The proposed reconstruction algorithm optimizes whole image region while the Poisson image editing only optimizes the source image region. The proposed fast Poisson reconstruction has a closed form solution and a color preserving parameter. This color preserving parameter can control the color adaptation level. If the color adaptation parameter is large, the color of the source

³The code is available at <http://www.ok.ctrl.titech.ac.jp/res/IC/IC.html>

and destination is perfectly preserving in the reconstructed result. In the proposed fast Poisson reconstruction, we minimize the following energy functional.

$$f[r] = \int_T |\nabla r - \mathbf{v}|^2 dt + \varepsilon \int_T |r - \tilde{r}|^2 dt, \quad (9)$$

where \tilde{r} is the naive composed image, T is the whole image region, and ε is the color preserving parameter. The closed form solution of Eq. (9) is derived from the functional derivative $\delta f[r]/\delta r$ as

$$(\text{div } \mathbf{v} - \Delta r) + \varepsilon(\tilde{r} - r) = 0. \quad (10)$$

The discretized version of Eq. (9) and Eq. (10) are given by

$$F(\{R_i\}) = \sum_i \|\nabla R_i - \mathbf{V}_j\|_{\tilde{r}}^2 + \varepsilon \sum_i \|R_i - \tilde{R}_i\|^2, \quad (11)$$

$$(U_i - \Delta R_i) + \varepsilon(R_i - \tilde{R}_i) = 0, \quad (12)$$

where R_i and \tilde{R}_i are discretized value of r and \tilde{r} at i -th pixel, \mathbf{V}_j is discretized value of \mathbf{v} , and U_i is the discretized version of $\text{div } \mathbf{v}$ at i -th pixel, respectively. It is worthy noting that the color version of the energy $F(\{R_i\})$ in Eq. (12) is equal to the energy $\tilde{E}_R(\{\mathbf{R}_i\}, \{\hat{\mathbf{v}}_i\})$ in Eq. (6). The solution of Eq. (12) is effectively obtained using discrete cosine transform as

$$R_\omega = \frac{U_\omega + \tilde{R}_\omega}{\varepsilon + L_\omega}, \quad (13)$$

where R_ω is the discrete-cosine-transformed reconstructed image of at the frequency ω , U_ω is the discrete-cosine-transformed component of U_i , \tilde{R}_ω is the discrete-cosine-transformed naive composed image, L_ω is the discrete-cosine-transformed Laplacian operator Δ .

Author Biography

Takashi Shibata received the B.S. and M.S. degrees from the Department of Physics, Tohoku university. in 2005 and 2007, respectively. He joined NEC Corporation in 2008. His research interests include image processing and pattern recognition. He is currently a Ph.D candidate in the Department of Control Engineering, Tokyo Institute of Technology.

Masayuki Tanaka received his bachelor's and master's degrees in control engineering and Ph.D. degree from Tokyo Institute of Technology in 1998, 2000, and 2003. He joined Agilent Technology in 2003. He was a Research Scientist at Tokyo Institute of Technology since 2004 to 2008. Since 2008, He has been an Associated Professor at the Graduate School of Science and Engineering, Tokyo Institute of Technology. He was a Visiting Scholar with Department of Psychology, Stanford University, CA, USA.

Masatoshi Okutomi received a B.Eng. degree from the Department of Mathematical Engineering and Information Physics, the University of Tokyo, Japan, in 1981 and an M.Eng. degree from the Department of Control Engineering, Tokyo Institute of Technology, Japan, in 1983. He joined Canon Research Center, Canon Inc., Tokyo, Japan, in 1983. From 1987 to 1990, he was a visiting research scientist in the School of Computer Science at Carnegie Mellon University, USA. In 1993, he received a D.Eng. degree for his research on stereo vision from Tokyo Institute of Technology. Since 1994, he has been with Tokyo Institute of Technology, where he is currently a professor in the Department of Mechani-

cal and Control Engineering, the Graduate School of Science and Engineering.